Application of Thixotropy to Analyze Fatigue and Healing Characteristics of Asphalt Binder

Liyan Shan, Yiqiu Tan, Shane Underwood, and Y. Richard Kim

The fatigue performance of asphalt binder is critical to understanding the fatigue performance of asphalt mixtures, especially the effects of healing. Although research into the fatigue and healing characteristics of asphalt binder is found in numerous references, an efficient technique to evaluate these characteristics still does not exist. Thixotropy is a concept that may help explain the material behavior and provide an efficient evaluation technique. This property is related to the breakdown and buildup of microstructure that may cause the changes observed during fatigue and healing tests. Thus, tracking the thixotropy of asphalt binders may be a good method to study fatigue and healing. For this study, experiments were performed to characterize the fatigue and healing characteristics of three typical asphalt binders. Then a common thixotropic model was characterized with a relatively simple stepped-flow test and oscillation experiment. The resulting model shows good correlation with the measured fatigue and healing tests. This finding, though based on a limited number of binders, suggests that thixotropy may play a role in the fatigue and healing characteristics of asphalt binder.

Fatigue degradation is one of the main failure modes of asphalt concrete pavement. The ability of asphalt binder to resist accumulation of this fatigue damage can profoundly affect the service life of asphalt pavements. It has long been observed that laboratory fatigue tests underestimate the fatigue life of actual in-service asphalt concrete pavements (*1*). One initial hypothesis for this underestimation is that laboratory tests do not capture the beneficial aspects of rest periods between loadings (*2*). Subsequent experiments to verify and quantify this hypothesis have resulted in a great deal of literature supporting the concept of healing for asphalt mixtures and, consequently, for asphalt binder (*3–8*). Healing can be defined as ability of a material to recover stiffness and strength lost through previous loadings; it should be interpreted as independent of any linear viscoelastic recovery.

Currently, the ability of asphalt binder and mixtures to heal is generally accepted as fact by researchers. Probably the first documented experimental evidence of asphalt concrete healing was provided by Deacon (*3*), who showed that the fatigue life of asphalt concrete can be extended when the duration of the rest period between loadings increases. Other researchers confirmed this basic observation by performing similar tests in direct tension fatigue mode (*4*). Some researchers have focused on trying to identify the material characteristics that affect the healing potential, using relatively simple indices. For example, Kim et al. performed beam fatigue experiments on asphalt sand mixtures while introducing rest periods of 5 to 40 min (*5*). Comparisons were then made between the pseudo strain energy density before and after the rest periods. The pseudo strain concept was introduced in this work as a means to separate the recovery related to viscoelastic processes from that related to actual microstructural healing mechanisms. Using an index defined with these energy density values, along with chemical analysis of the asphalt binder, Kim et al. showed a correlation between healing potential of the mixture and chemical composition of the asphalt binder. Little et al. performed flexural beam fatigue experiments with rest periods up to 24 h and noted that the fatigue life was extended in excess of 100% for some materials (*6*). Kim et al. (*7*) performed torsional fatigue tests on sand asphalt samples with rest periods and quantified the effect of healing time using a pseudo-based analysis similar to that of others (*1, 5*). Breysse et al. used the damage rate, a hyperbolic kinetics-based index, as an indicator of the effect of loading history on healing potential (*8*). Carpenter and Shen used the ratio of dissipated energy at failure and the so-called plateau value (PV) to quantitatively characterize the effects of rest periods on fatigue life (*9*). Pronk also used energy-based principles to establish a partial healing model for asphalt mixtures (*10, 11*).

These research efforts have focused on healing of asphalt mixtures, but some were able to isolate the importance of asphalt binder and mastic in the healing process (*6, 7, 12*). Planche et al. used a dynamic shear rheometer (DSR) to directly evaluate the fatigue and healing properties of asphalt binder (*13*). These researchers subjected asphalt samples to continuous loading and then introduced rest periods of 40 min or 6 h and remeasured the material response. The conclusion of this work is that rest periods can significantly affect the material response, especially when introduced before failure. Bahia et al. performed strain sweep tests with rest periods of 12 h and found that the behavior before and after the rest period was similar (*14*). This finding suggests that most of the modulus loss that occurs due to loading recovers over time. Finally, Shen et al. (*15*) followed the PV approach used in mixture evaluation (*9*) to study the fatigue and healing of binder, and they found trends similar to those observed in mixture testing.

This previous research is useful in providing evidence of healing, evaluating the effects of various factors on the magnitude of healing, and ranking the healing properties of various binders. However, the healing mechanism itself is not clearly understood. Yet it seems to be the key to understanding the fatigue and healing characteristics

L. Shan, 202 Haihe Road, and Y. Tan, 73 Huanghe Road, School of Transportation Science and Engineering, Harbin Institute of Technology, Nangang District, Harbin 150090, China. S. Underwood, 216C Mann Hall, and Y. R. Kim, 210 Mann Hall, Department of Civil, Construction, and Environmental Engineering, North Carolina State University, 2501 Stinson Drive, Raleigh, NC 27695-7908. Corresponding author: L. Shan, myshanliyan@126.com.

Transportation Research Record: Journal of the Transportation Research Board, No. 2179, Transportation Research Board of the National Academies, Washington, D.C., 2010, pp. 85–92.
DOI: 10.3141/2179-10

of asphalt binder. Motivated by micromechanical models, researchers have measured the surface energies of asphalt binder and found good correlation between these properties and the healing and fatigue propensity of different materials (*16, 17*). Bhasin et al. developed a model to describe the healing of asphalt binder based on a convolution of wetting and intrinsic healing processes (*18*). Bommavaram et al. demonstrated ways that the DSR could be used to determine the parameters of this intrinsic healing function (*19*). These researchers characterized asphalt binder using different and known healing properties. Based on their research, healing occurs first via wetting and then interfacial cohesion and interdiffusion of the molecules between the wet surfaces.

This framework proposed by Bhasin et al. seems to have captured an underlying fundamental characteristic of asphalt binder, and it conceptually explains many of the findings in the aforementioned studies (*18*). However, Bhasin et al.'s work is not the only potential interpretation of fatigue and healing. One concept receiving attention with regard to asphalt behavior is thixotropy. Thixotropy is defined as the continuous decrease of viscosity (or of material properties generally) with time when a sample, previously at rest, is subjected to flow. Thixotropy also refers to the subsequent recovery of those material properties with time when the flow is discontinued (*20*). This behavior is not to be confused with the linear viscoelastic behaviors of creep and relaxation, which are also known to have a significant effect on the asphalt response. The thixotropic mechanism differs from linear viscoelastic behavior because it becomes important only at high input levels, for example, outside the linear viscoelastic range. This mechanism is one of the oldest documented rheological phenomena in the colloidal sciences. Much has been written on the topic with regard to effective test methods and useful models. In particular, the efforts of Moore (*21*), Cheng and Evans (*22*), and Mewis and Wagner (*20*) apply to the study at hand.

Thixotropy is related to the changes in microstructure of the material. By shearing, the microstructure breaks down (but not necessarily in the form of cracking), and viscosity decreases. After a period of rest, it is possible for the material to regain the broken-down structure and again show the initial value of the viscosity due to the specific Brownian motion of its molecules. Thixotropy is different from the concept of shear thinning, which also has been applied to describe non-Newtonian behavior of asphalt cements at high temperatures (*23, 24*). Shear thinning is the decrease in viscosity with an increase in shear rate. The dependence on shear rate, as opposed to time, differentiates the two mechanisms. Because fatigue and healing vary in time, it is believed that thixotropy is the proper parameter to describe their evolution. Even though the processes are time dependent, some research has shown that the thixotropic nature of a material can result in structural changes during oscillation cycles (e.g., in frequency domain), as well as in long transients (*20, 25*). This dual dependence suggests that thixotropy can affect the fatigue and healing of asphalt binder subjected to oscillatory loading. If these findings apply to asphalt binder, then thixotropy may be a useful tool to analyze fatigue and healing of asphalt binder.

This concept is not entirely new for interpreting asphalt fatigue and healing behavior. Soltani and Anderson used uniaxial push–pull tests to research fatigue and healing, and they concluded that the modulus lost during a fatigue test and the modulus gained during rest periods are the result of thixotropy (*26*). Apart from this work, though, little research has been directed toward ways that thixotropy affects the performance of asphalt binder. In this study, the fatigue and healing characteristics of a few selected binders are determined and interpreted within a thixotropic framework.

OBJECTIVE

The objective of this study is to determine if the concept of thixotropy can be applied to interpret and predict fatigue and healing characteristics of asphalt binder.

PROPOSED METHODOLOGY

Asphalt binder fatigue is usually researched in oscillation mode, and the dynamic shear modulus, $|G^*|$, is the main material property used to evaluate the material characteristics. For thixotropy, viscosity is the main parameter used to reflect structural changes. In a non-Newtonian fluid, such as asphalt binder, thixotropy can be considered by using dynamic viscosity, $|\eta^*|$. This parameter is closely related to the $|G^*|$, but it is more commonly used because it can be related directly to steady-state viscosity through the Cox–Merz relationship (*27*).

The Cox–Merz relationship is an empirical one of great use in rheology. Cox and Merz were the first to observe that for many polymeric systems, a correspondence occurs between steady-state shear viscosity, η, at some shear rate, and the magnitude of $|\eta^*|$, at an angular frequency, ω, equal to that same shear rate, in Equation 1. For example, the Cox–Merz rule would suggest that η at 62.8 γ/s is equal to $|\eta^*|$ from an oscillation test conducted at 62.8 rad/s (10 Hz). This phenomenon is useful because of experimental difficulties in directly measuring η at high shear rates.

$$|\eta^*(\omega)| = \eta(\dot{\gamma}) \tag{1}$$

Many researchers define a state variable, λ, to track microstructural changes. The general form of the evolution law for this parameter is shown in Equation 2 and consists of two terms: buildup and breakdown. When λ equals 1, a completely built-up structure is said to exist, whereas when λ equals 0, a completely broken-down structure exists. In Equation 2, the rate of change of the microstructure is a function of the current microstructural state, shear rate, and material-defined coefficients (a, b, c, and d). The part of this equation containing coefficients a and c is the buildup term, and the part containing coefficients b and d is the breakdown term. From this equation, it can be seen that buildup and breakdown are directly proportional to coefficients a and b, respectively. This observation is stated later in this paper.

$$\frac{d\lambda}{dt} = a(1-\lambda)^c - b\lambda\dot{\gamma}^d \tag{2}$$

where

λ = state variable;
a, c = coefficients related to microstructural buildup;
b, d = coefficients related to microstructural breakdown; and
$\dot{\gamma}$ = shear rate.

Researchers using this general form have followed various specific models. For example, Moore (*21*) made both c and d unity, Cheng and Evans (*22*) made d unity but allowed c to be non-unitary, and Mewis and Wagner (*20*) set both powers equal to non-unitary values. In this study, the model suggested by Cheng and Evans (*22*) is used, that is, Equation 3.

$$\frac{d\lambda}{dt} = a(1-\lambda)^c - b\lambda\dot{\gamma} \tag{3}$$

MATERIALS AND TEST METHODS

Three PG 70-22 asphalt binders were selected for this study. For the remainder of this paper, these materials are labeled as generic Binders A, B, and C. All are standard, unmodified asphalt materials. Binders B and C come from the same source but sampled at different times, and Binder A comes from a completely different source. These binders were all aged in a rolling thin-film oven before testing, to simulate the effect of mixing and compaction. Laboratory testing was performed using a TA Instruments AR-G2 Rheometer. Four types of test were conducted: frequency sweep, controlled-stress fatigue, healing, and flow. All tests were conducted with an 8-mm diameter parallel plate geometry and 2-mm gap setting.

Frequency Sweep Test

Frequency sweep tests were conducted for frequencies from 0.1 Hz to 30 Hz and for temperatures of 10°, 16°, 19°, 22°, 25°, and 30°C. This combination of temperatures and frequencies ensures sufficient overlap in the material responses so that the data could be horizontally shifted to obtain master curves of the key properties. Before performing these frequency sweep tests, a stress sweep was conducted
Fig. 1 (Figure 1*a*) to ensure that all frequency sweep tests were conducted in the linear range.

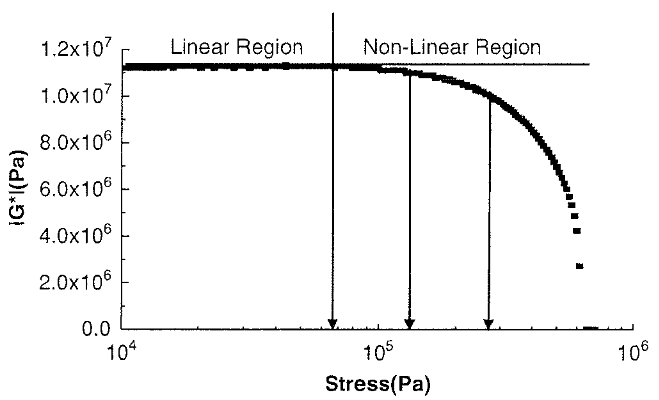

(a)

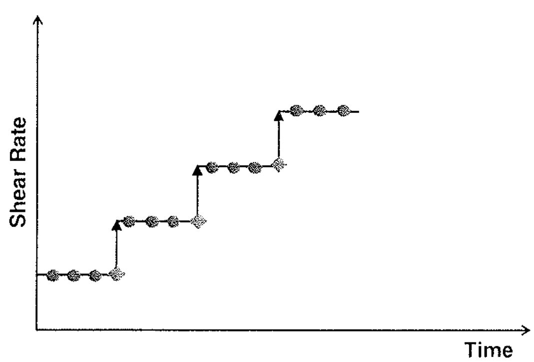

(b)

FIGURE 1 (*a*) Stress level selection from stress sweep and (*b*) schematic of steady-state flow test and stepped-flow test.

Fatigue Test

Fatigue tests were conducted in controlled stress mode with a 10-Hz continuous sinusoidal loading until the $|\eta^*|$ was equal to 50% of the $|\eta^*|$ at cycle 10. Stress levels for these experiments were chosen from results of the same stress sweep test used in establishing the linear viscoelastic limits of the material, as shown in Figure 1*a*. Three stress levels were chosen for testing, diagrammed in Figure 1*a*. Because fatigue is generally a concern at intermediate temperatures, tests were conducted at 25°C and 20°C. At least three replicates were performed for each condition, and results presented in this paper are the arithmetic average of the replicates. Although not shown in this paper, the variability for these tests was generally less than 10%.

Healing Test

Healing tests consist of an initial fatigue test, with the exception that the terminal $|\eta^*|$ value changes, followed by a rest period, and then finally another fatigue test. To evaluate the effectiveness of healing at different microstructural configurations, three terminal $|\eta^*|$ values were chosen: 20%, 40%, and 60% of the initial values. Five rest periods were used in this testing: 1 h, 6 h, 12 h, 24 h, and 48 h. Only a single stress level, 4×10^5 Pa, and temperature, 25°C, were used.

Flow Test

Two kinds of flow tests were conducted in this research: steady-state flow and stepped flow. Both tests are similar, and in each, the material is subjected to a constant shear rate for a given time until it is increased to another level. Differences between the two protocols exist in the size of the shear rate step and in the times at which the material properties are assessed. A diagram of the basic protocol for both tests is given in Figure 1*b*. The steady-state flow test is represented in this figure by filled diamonds, and the stepped-flow protocol is represented by filled circles.

The purpose of steady-state flow tests is to establish a relationship between η and shear rate. To cover the necessary range of conditions, shear rates are gradually stepped up from 1×10^{-5} to 10 γ/s. Each rate is maintained until steady-state flow is achieved. The steady state is determined automatically by data acquisition software when the change in η for three consecutive data points is less than 5%. The property of interest is this steady-state η. The stepped-flow test is used to characterize the thixotropic model shown in Equation 3. Three shear rates were used—0.01, 0.1, and 1 γ/s—and the entire time history for each shear rate was acquired. Stepped-flow tests were conducted only at 25°C.

RESULTS AND ANALYSIS

Dynamic Viscosity of Binder in Fatigue Tests

The fatigue characteristics of asphalt binder are affected by many factors, including chemical composition, temperature, loading level, and so on. In this study, three stress levels were used to gain insight into fatigue performance of the chosen binders. Typical results from these tests are shown in Figure 2 in regard to $|\eta^*|$ versus cycle number Fig. 2

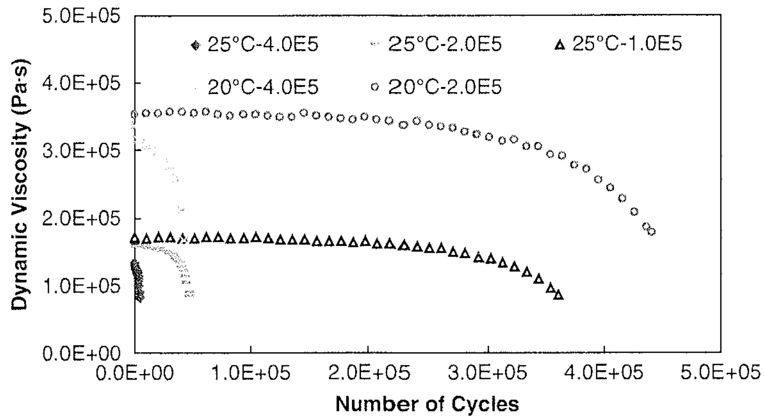

FIGURE 2 Dynamic viscosity of Binder A in selected fatigue tests.

for Binder A. Responses for the different temperatures and input conditions are shown also in this figure.

It is seen in all cases that $|\eta^*|$ decreases slowly at first, but then the degradation accelerates quickly as the specimen approaches failure. Failure in these experiments is determined when $|\eta^*|$ reaches 50% of its value at cycle 10. From Figure 2, it is also seen that the fatigue life is shortened with increased input magnitude and also with an increase in temperature; both results are expected, based on experience with controlled stress experiments.

Tab. 1 Table 1 summarizes the fatigue behavior of each asphalt binder at different input levels and temperatures. This table shows that Binder A outperforms both Binders B and C, and that Binder B outperforms Binder C. The difference between Binder A and Binder B is greater than the difference between Binder B and Binder C. An interesting observation from Table 1 is that although Binder A performs better under all fatigue conditions, the relative ranking differs for each test condition. For example, at 25°C and 4×10^5 Pa stress level, the percentage of difference between Binder A and Binder B is approximately 54%, whereas at 25°C and 1×10^5 Pa, it is only 34%.

Dynamic Viscosity of Binder in Healing Tests

The healing characteristics of asphalt binder are known to be affected by temperature, time, and material condition when a rest period is introduced. The healing experiments in this study focus on the latter two factors only. Typical results are shown in Figure 3*a* for the case where a healing period is introduced after $|\eta^*|$ reaches 20% of its initial value. Figure 3*b* shows typical results when a healing period is introduced after $|\eta^*|$ reaches 60% of its initial value. Results from multiple test specimens are shown in each of these figures. The data Fig. 3

TABLE 1 Fatigue Life of Study Binders

Binder	Temperature (°C)	Stress Level (Pa)	Fatigue Life
A	25	4.0E+05	4,402
		2.0E+05	51,495
		1.0E+05	382,781
	20	4.0E+05	42,356
		2.0E+05	451,435
B	25	4.0E+05	2,000
		2.0E+05	25,144
		1.0E+05	249,875
	20	4.0E+05	22,168
		2.0E+05	221,396
C	25	4.0E+05	1,553
	20	4.0E+05	21,789

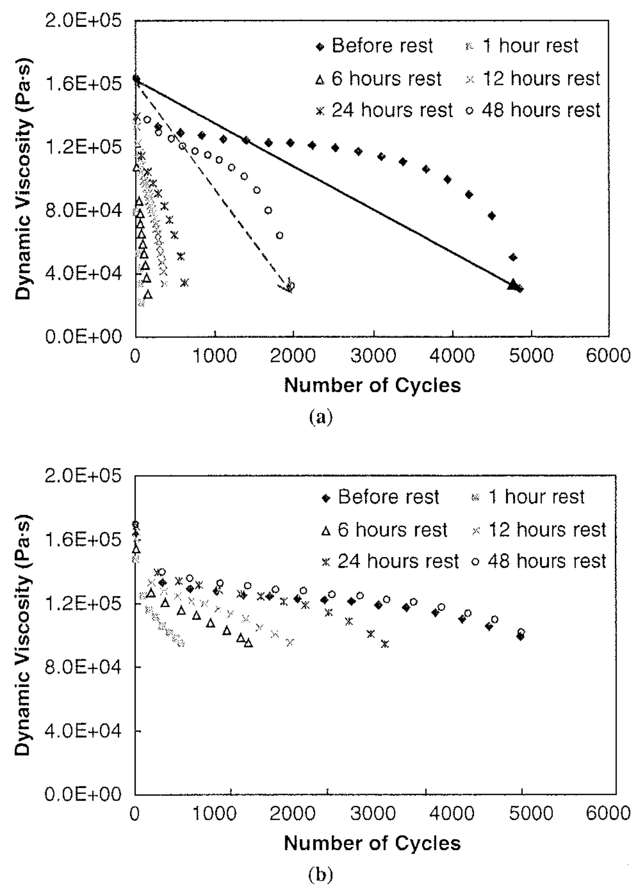

FIGURE 3 Dynamic viscosity degradation of Binder A with different rest periods for (*a*) 20% terminal $|\eta^*|$ case and (*b*) 60% terminal $|\eta^*|$ case.

series that have labels ending with rest have been tested previously to either 20% (Figure 3*a*) or 60% (Figure 3*b*) of the initial $|\eta^*|$. Thus, for these series, the *x*-axis is actually the number of cycles after each rest period. To simplify Figure 3*a* and 3*b*, only a single before rest curve is shown. Each curve corresponds to the average of the three experiments. Virgin degradation curves are not shown for each of these cases because they are the same as the before rest curve. It is seen from these two parts of the figure that a longer rest period results in more recovery of the initial $|\eta^*|$ and a more gradual degradation of the $|\eta^*|$. However, in the case of 20% reduction, even 48 h is not enough time for full healing. This is not the case with the 60% reduction experiments, which show that after 48 h of rest, the reloaded sample yields essentially the same behavior as for the virgin sample. The slight disagreement in the 48 h rest and before rest series in Figure 3*b* can be attributed to specimen-to-specimen variability.

To better quantify the effect of rest period and material state on $|\eta^*|$ recovery, a damage rate index similar to that proposed by others (*6, 19*) has been evaluated. Referred to as the damage rate, *D*, it is calculated directly from the $|\eta^*|$ degradation plots. The *D* is defined mathematically in Equation 4 and shown graphically for the after rest series as a dashed arrowed line in Figure 3*a* and for the before rest series as a solid arrowed line. A larger *D* means that the $|\eta^*|$ degrades at a quicker rate. In regard to thixotropy, this phenomenon may be interpreted as a more rapid breakdown in microstructure.

$$D_i = \frac{|\eta^*|_1 - |\eta^*|_{\text{terminal}}}{N} \tag{4}$$

where

D_i = damage rate at terminal $|\eta^*|_i$,
$|\eta^*|_1$ = dynamic viscosity immediately after recovery (Pa · s),
$|\eta^*|_{\text{terminal}}$ = dynamic viscosity immediately before recovery (Pa · s), and
N = number of cycles required to reduce dynamic viscosity from $|\eta^*|_1$ to $|\eta^*|_{\text{terminal}}$.

The *D* is computed for each $|\eta^*|$ degradation curve and compared with the *D* for the virgin specimen to quantify the effects of the rest periods. The resulting index, termed the healing index (HI), provides a snapshot of the effectiveness of a given rest period for rebuilding microstructure. The index is defined mathematically in Equation 5. In this equation, the subscript *N*, which follows HI, is used to differentiate among the healing indices computed from the tests conducted to different terminal $|\eta^*|$ values. The index value may range from 0 to 100, with 0 representing no recovery and 100 representing complete recovery. As an example, in Figure 3*a*, the dashed line represents *D* for a rest period of 48 h and a terminal $|\eta^*|$ of 20% virgin values, and the solid line represents *D* for the initial fatigue cycles. The healing index for this condition, denoted as $HI_{20}(48)$, would equal the ratio of the slopes of the solid and dashed lines. In this case, the ratio is 38.9%. Results for all of the binders and test conditions are summarized in Table 2. Tab. 2

$$HI_N = \frac{D_{\text{before rest}}}{D_{\text{after rest}}} * 100 \tag{5}$$

The major trend found from Table 2 is that the HI improves for all binders with increased healing time. It is also seen that for the same rest period, but more extreme terminal $|\eta^*|$, the healing decreases, thus indicating that the healing rate is damage level dependent. Taking the slope of the relationship between HI and terminal $|\eta^*|$ as an indicator of this sensitivity suggests that microstructural changes occurring from 40% to 60% initial $|\eta^*|$ are relatively more critical in Binders B and C than they are in Binder A. For example, applying a 1-h rest period for Binder A in the 60% case increases the HI approximately 5% relative to the 40% experiment, but for Binders B and C, the increase is almost 10%. Also seen is that, based on the HI, Binder A is better overall at regaining its microstructural configuration than both Binders B and C. The exception to this case is for relatively short rest periods in the 60% and 40% cases. Somewhere between the 12- and 24-h marks, Binder A shows a rapid recovery in microstructural properties. This rapid improvement does not occur for either Binder B or C.

TABLE 2 Healing Results of Study Binders

Binder	Temperature (°C)	Healing Time (h)	HI_{20}	HI_{40}	HI_{60}
A	25	1	4.3	9.1	14.1
		6	6.1	15.2	26.0
		12	8.5	21.1	35.8
		24	17.1	37.5	59.4
		48	38.9	56.9	85.1
B	25	1	4.0	12.8	22.4
		6	5.7	17.2	32.5
		12	6.3	22.7	47.9
		24	8.3	26.6	52.5
		48	20.0	41.3	63.0
C	25	1	6.3	14.3	23.1
		48	—	40.0	61.9

Applicability of Cox–Merz Relationship

To use existing thixotropic models, it is important to characterize the zero shear viscosity, η_0, and infinite viscosity, η_∞. Unfortunately, as discussed earlier, it is impossible to obtain the flow curve at very high shear rate rates with the available equipment. This problem is solved by using the Cox–Merz relationship to combine results of the frequency sweep and steady-state flow tests. However, because this relationship is empirical, it must first be confirmed that it applies for asphalt binder over the range of conditions encountered. For analysis, the frequency sweep results, $|\eta^*|$ as a function of frequency at different temperatures, were first combined into a single functional relationship by using the principle of time–temperature superposition (*27, 28*). A representative sample of the resulting $|\eta^*|$ master curve is shown in Figure 4*a*. Similarly, results from the steady-state flow tests conducted at different temperatures were combined into a single master curve of η as a function of shear strain rate. Finally, the Cox–Merz relationship, Equation 1, was used to translate the frequency sweep data into the shear rate space and to develop a complete flow curve. The combined curve is shown, along with the best-fit Carreau viscosity relationship Equation 6 and in Figure 4*b*. Although results for only a single binder are shown, results for the other binders are similar. Fig. 4

$$\frac{\eta - \eta_\infty}{\eta_0 - \eta_\infty} = \left\{1 + (\alpha\dot{\gamma})^2\right\}^{(n-1)/2} \tag{6}$$

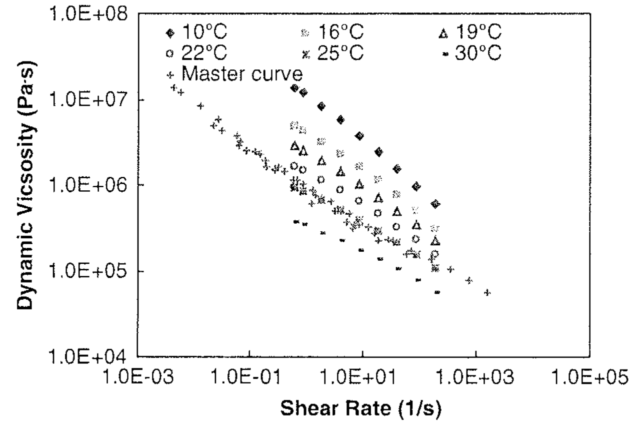

(a)

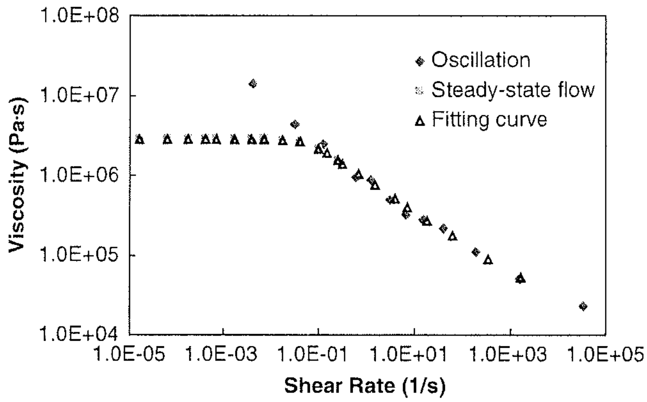

(b)

FIGURE 4 Use of time–temperature superposition principle and Cox–Merz relationship to create complete flow curve: (a) frequency sweep data and (b) combined frequency sweep and steady-state flow data.

where

η_∞ = infinite viscosity (Pa · s),
η_0 = zero shear viscosity (Pa · s),
$\dot{\gamma}$ = shear rate, and
α, n = regression coefficients.

The combined frequency sweep and steady-state shear data confirm that the Cox–Merz relationship is reasonable for many conditions, but it does not apply below an angular frequency of approximately 1×10^{-1} rad/s (for a reference temperature of 25°C). For the purposes of this study, frequency sweep data at angular frequencies below approximately 1×10^{-1} rad/s are not included when developing the flow master curve and when characterizing Equation 6. The resultant η_0, η_∞, n, and α parameters are shown in Table 3 for each of the study binders. Tab. 3

Thixotropy of Asphalt Binder

For simplicity of characterization, the microstructural state variable, λ, is assumed to be equal to the normalized viscosity, Equation 7, where η_∞ and η_0 have been determined from the flow master curve. Equation 7 can be used along with the measured viscosity from the stepped-flow test to compute λ as a function of time, which can then be numerically differentiated, substituted into Equation 2, and regressed to find the values of Coefficients a, b, and c.

$$\lambda = \frac{\eta(t) - \eta_\infty}{\eta_0 - \eta_\infty} \tag{7}$$

Through theory related to thixotropy, the Cheng and Evans model parameters a and b are related directly to the mechanisms leading to healing and loss in fatigue, respectively. High values of coefficient a mean that a material should recover its microstructure (i.e., heal) better, whereas high values of coefficient b mean that a material loses microstructure (i.e., becomes damaged) more easily. If it can be shown that these parameters correlate with the physically observed fatigue and healing characteristics, then it suggests that thixotropy may have a role in the behavior of asphalt binder. The ranking of the coefficients and of each binder in fatigue and healing is shown in Figure 5. Figure 5a and 5b show the coefficients from the model. Fig. 5
Figure 5c shows the HI for the 60% $|\eta^*|$ case after 48 h of rest, and Figure 5d shows results from fatigue tests performed at a level of 4×10^5 Pa and at 25°C.

First, it is observed that, generally, the rankings of the coefficients and the material responses agree. Coefficient b suggests a ranking of Binder A, then Binder B, and then Binder C. It also suggests that differences between Binder A and Binders B and C are larger than the difference between Binders B and C. Both of these trends are also observed in the binder fatigue tests, as indicated in Figure 5d. To match the trend from Coefficient a, the HI was examined for a long rest period. Short rest period results do not coordinate as well with the a coefficient. This condition may mean that the a coefficient alone is representative of only the ultimate recovery potential of the material. When a is adjusted by raising it to the power of c (see Table 3), then the resulting combined parameter does rank the materials for short rest periods.

CONCLUSIONS AND FUTURE WORK

This paper compares the fatigue and healing characteristics of three different asphalt binders for different input conditions. Results are first interpreted using the observed responses in combination with

TABLE 3 Thixotropic Model Coefficients

Binder	η_0 (Pa · s)	η_∞ (Pa · s)	α	n	a	b	c	a^c
A	2.79×10^6	9,647	16.64	0.5875	8.44×10^6	0.0178	−0.437	165
B	1.93×10^6	7,329	12.98	0.5960	5.62×10^6	0.0250	−0.546	733
C	2.09×10^6	7,405	13.55	0.5938	4.46×10^6	0.0272	−0.547	848

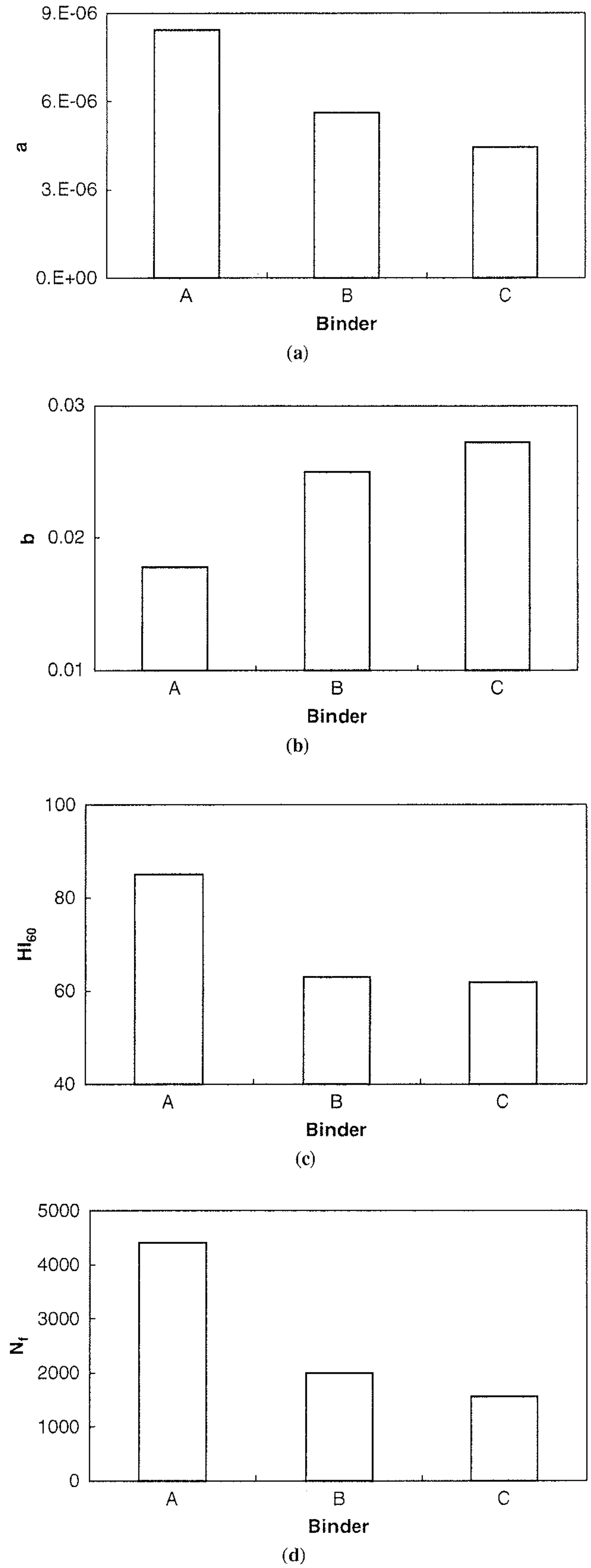

FIGURE 5 Relationship between fatigue and healing response and thixotropic coefficients; (*a*) buildup Coefficient a, (*b*) breakdown Coefficient b, (*c*) healing, and (*d*) N_f.

specific indices. Next, a thixotropic model is characterized and used to gain insight into the underlying processes leading to the observed responses. From results presented, several conclusions can be drawn:

1. Asphalt binder performance becomes worse under continued, repeated loading. Under controlled stress loading, high load levels and high temperatures yield poor performance.
2. Asphalt binder performance improves after a rest period. Longer rest periods always yield more improvement, although the specific effect depends on the material and on the microstructural configuration immediately before the rest period began.
3. The Cox–Merz relationship can be applied to asphalt binder to a temperature–frequency combination that approximately equals 1×10^{-1} rad/s at 25°C.

In addition to these conclusions, and based on the limited number of asphalt binders presented in this paper, some relationship seems to exist between the thixotropic model parameters and observed material behavior. To confirm these findings and gain additional substantiation of the importance of thixotropic processes, a comprehensive study that uses a set of asphalt binders that exhibits a wider range of fatigue and healing characteristics is needed. Such a study should include asphalt binders that are known from other studies to show extreme differences in healing and fatigue. The results of such a study potentially could lead to a screening test threshold to quickly identify good- and poor-performing materials.

ACKNOWLEDGMENTS

This study was sponsored by the National Natural and Science Foundation of China and the China Scholarship Council.

REFERENCES

1. Finn, F., C. L. Saraf, R. Kulkarni, K. Nair, W. Smith, and A. Abdullah. *NCHRP Report 291: Development of Pavement Structural Subsystems.* TRB, National Research Council, Washington, D.C., 1986.
2. Lytton, R. L., J. Uzan, E. G. Fernando, R. Roque, D. Hiltunen, and S. M. Stoffels. *SHRP-A-357: Development and Validation of Performance Prediction Models and Specifications for Asphalt Binders and Paving Mixtures,* TRB, National Research Council, Washington, D.C., 1993.
3. Deacon, J. A. *Fatigue of Asphalt Concrete.* PhD dissertation. University of California, Berkeley, 1965.
4. Raithby, K. D., and A. B. Sterling. The Effect of Rest Periods on the Fatigue Performance of a Hot-Rolled Asphalt Under Repeated Loading. *Journal of the Association of Asphalt Paving Technologists,* Vol. 39, 1970, pp. 134–152.
5. Kim, Y. R., D. N. Little, and F. C. Benson. Chemical and Mechanical Evaluation on Healing Mechanism of Asphalt Concrete. *Journal of the Association of Asphalt Paving Technologists,* Vol. 59, 1990.
6. Little, D. N., R. L. Lytton, A. D. Williams, and C. W. Chen. *Microdamage Healing in Asphalt and Asphalt Concrete, Vol. I: Microdamage and Microdamage Healing.* Project Summary Report. FHWA-RD-98-144. Texas Transportation Institute, Texas A&M University System, College Station, Tex., 2001.
7. Kim, Y. R., D. N. Little, and R. L. Lytton. Fatigue and Healing Characterization of Asphalt Mixtures. *Journal of Materials in Civil Engineering,* Vol. 15, 2003, pp. 75–83.
8. Breysse, D., C. De La Roche, V. Domec, and J. J. Chauvin. Influence of Rest Time on Recovery and Damage During Fatigue Tests on Bituminous Composites. *Materials and Structures,* Vol. 36, 2003, pp. 648–651.
9. Carpenter, S. H., and S. Shen. Dissipated Energy Approach to Study Hot-Mix Asphalt Healing in Fatigue. In *Transportation Research Record:*

Journal of the Transportation Research Board, No. 1970, Transportation Research Board of the National Academies, Washington, D.C., 2006, pp. 178–185.
10. Pronk, A. C. Partial Healing: A New Approach for the Damage Process During Fatigue Testing of Asphalt Specimen. *Proc., ASCE Symposium on Mechanics of Flexible Pavements.* Baton Rouge, La., 2006.
11. Pronk, A. C. PH Model in 4PB Test with Rest Periods. *Road Materials and Pavement Design,* Vol. 10, 2009, pp. 417–426.
12. Lee, H. J., and Y. R. Kim. A Viscoelastic Continuum Damage Model of Asphalt Concrete with Healing. *Journal of Engineering Mechanics,* ASCE, Vol. 124, 1998, pp. 1–9.
13. Planche, J.-P., D. A. Anderson, G. Gauthier, Y. M. Le Hir, and D. Martin. Evaluation of Fatigue Properties of Bituminous Binders. *Materials and Structures,* Vol. 37, 2004, pp. 356–359.
14. Bahia, H., H. Zhai, K. Bonnetti, and S. Kose. Non-Linear Viscoelastic and Fatigue Properties of Asphalt Binders. *Journal of Association of Asphalt Paving Technologists,* Vol. 68, 1999, pp. 1–34.
15. Shen, S., H.-M. Chiu, and H. Huang. Fatigue and Healing in Asphalt Binders. Presented at 88th Annual Meeting of the Transportation Research Board, Washington, D.C., 2009.
16. Hefer, A. W., A. Bhasin, and D. N. Little. Bitumen Surface Energy Characterization Using a Contact Angle Approach. *Journal of Materials in Civil Engineering,* Vol. 18, 2006, pp. 759–767.
17. Bhasin, A. and D. N. Little. Characterization of Aggregate Surface Energy Using the Universal Sorption Device. *Journal of Materials in Civil Engineering,* Vol. 19, 2007, pp. 634–641.
18. Bhasin, A, D. N. Little, R. Bommavaram, and K. Vasconcelos. A Framework to Quantify the Effect of Healing in Bituminous Materials Using Materials Properties. *Road Materials and Pavement Design,* Vol. 9, 2008, pp. 219–242.
19. Bommavaram, R. R., A. Bhasin, and D. N. Little. Use of Dynamic Shear Rheometer to Determine Intrinsic Healing Properties of Asphalt Binders. Presented at 88th Annual Meeting of the Transportation Research Board, Washington, D.C., 2009.
20. Mewis, J., and N. J. Wagner. Thixotropy. *Advances in Colloid and Interface Science,* 2009, pp. 214–227.
21. Moore, F. The Rheology of Ceramic Slips and Bodies. *Transactions of the British Ceramic Society,* Vol. 58, 1959, pp. 470–494.
22. Cheng, D. C. H., and F. Evans. Phenomenological Characterization of Rheological Behaviour of Inelastic Reversible Thixotropic and Anti-thixotropic Fluids. *British Journal of Applied Physics,* Vol. 16, 1965, pp. 1599–1617.
23. Moisés, G. M., P. Partal, F. J. Navarro, F. Martínez-Boza, M. R. Mackley, and C. Gallegos. The Rheology of Recycled EVA/LDPE Modified Bitumen. *Rheological Acta,* Vol. 43, 2004, pp. 482–490.
24. Polacco, G., J. Stastna, Z. Vlachvicova, D. Biondi, and L. Zanzotto. Temperatory Networks in Polymer-Modified Asphalts. *Polymer Engineering and Science,* Vol. 44, 2004, pp. 2185–2193.
25. Srinivasa, R. R., and S. A. Khan. Shear-Induced Microstructural Changes in Flocculated Suspensions of Fumed Silica. *Journal of Rheology,* Vol. 139, 1995, pp. 1311–1325.
26. Soltani, A., and D. A. Anderson. New Test Protocol to Measure Fatigue Damage in Asphalt Mixtures. *Road Materials and Pavement Design,* Vol. 6, 2005, pp. 485–514.
27. Cox, W. P., and E. H. Merz. Correlation of Dynamic and Steady Flow Viscosities. *Journal of Polymer Science,* Vol. 28, 1958, pp. 619–622.
28. Ferry, J. D. *Viscoelastic Properties of Polymers.* John Wiley and Sons, Inc., New York, 1961.

The Characteristics of Bituminous Materials Committee peer-reviewed this paper.